

the observed and model resistivity curves to a minimum and is determined by trial and error.

The starting model is used to generate a theoretical synthetic sounding curve which is compared with the field data. An iterative process is then carried out to adjust the resistivities of the model while keeping the boundaries fixed. After each iteration the theoretical curve is recalculated and compared with the field data. This process is repeated until the RMS difference between the two curves reaches a minimum (Figure 7.33).

Zohdy's method has been developed by Barker (1992) for the inversion of SSI apparent resistivity pseudo-sections and more recently by using a deconvolution method (Barker, personal communication). Consequently, it is possible to produce fully automated

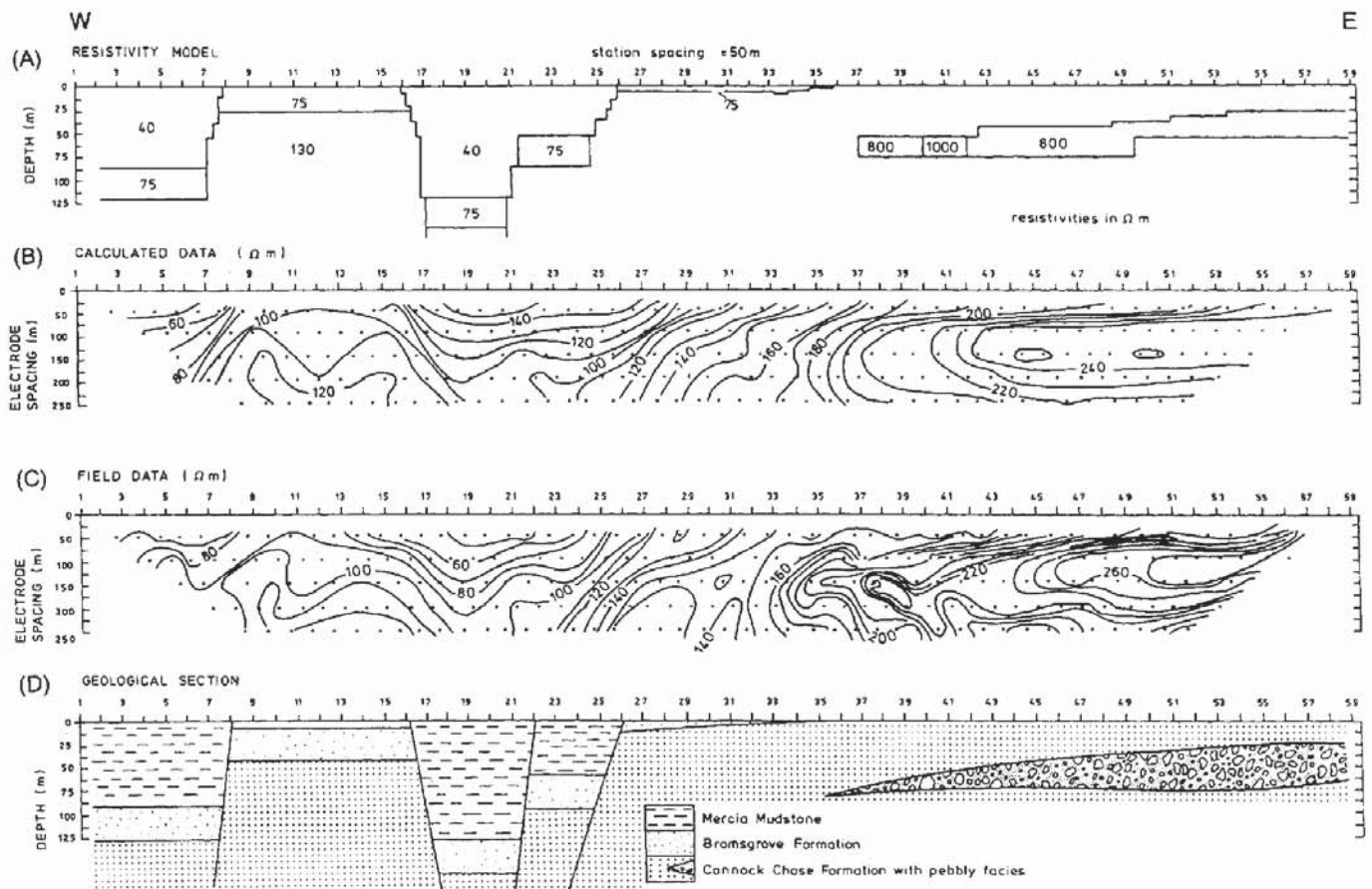
Figure 7.33 Automatic sounding inversion technique. (A) Observed data and initial layering. (B) Shifted layering and resulting model sounding curve. The difference (e) between the model and observed curves is used to apply a correction (c) to the layering. (C) The final layering and resulting model curve that is closely similar to the observed data. From Barker (1992), by permission

inversions of SSI pseudo-sections. The final results are displayed also as pseudo-sections in terms of the variations in true resistivity with depth as a function of distance along the array. Examples of inverted pseudo-sections are given in Section 7.7.

In addition to the above inversion routines, others have been produced, often in association with particular equipment, and also as specific developments of true tomographic imaging (e.g. Shima 1990; Daily and Owen 1991; Noel and Xu 1991; Xu and Noel 1993). Commercially available imaging inversion packages are available from a number of sources and are related to a style of data acquisition and equipment. Packages vary from those which can operate easily on a laptop computer, more sophisticated processing may require the computational power of a workstation with full colour plotting facilities.

Finite-element forward modelling can be undertaken using commercially available software. The resistivity response for a two-dimensional model is calculated and displayed as a pseudo-section for comparison with the original field data. This approach is used to help generate realistic sub-surface geometries in definable model structures (e.g. Figure 7.34).

Figure 7.34 Final interpretation of faulted Triassic sequence in Staffordshire, UK. (A) Two-dimensional finite difference model. (B) Computed apparent resistivity pseudo-section. (C) Field data. (D) Geological interpretation based on (A) and additional information. From Griffiths *et al.* (1990), by permission



7.6 MISE-À-LA-MASSE METHOD

The mise-à-la-masse or 'charged-body potential' method is a development of the CST technique but involves placing one current electrode within a conducting body and the other current electrode at a semi-infinite distance away on the surface (Figure 7.35). The voltage between a pair of potential electrodes is measured with appropriate corrections for any self-potentials.

For an isolated conductor in a homogeneous medium, the lines of equipotential should be concentric around the conductor (Figure 7.36A). In reality, lines of equipotential are distorted around an irregularly shaped conductive orebody (Figure 7.36B) and can be used to delimit the spatial extent of such a feature more effectively than using the standard CST method. The mise-à-la-masse method is particularly useful in checking whether a particular conductive mineral-show forms an isolated mass or is part of a larger electrically connected orebody. In areas where there is a rough topography, terrain corrections may need to be applied (Oppliger 1984). There are no general rules that can be applied to mise-à-la-masse data. Each survey is taken on its own merits and a plausible model constructed for each situation, although Eloranta (1984), for example, has attempted to produce a theoretical model to account for the observed potential distributions.

There are two approaches in interpretation. One uses the potential only and uses the maximum values as being indicative of the conductive body. The other converts the potential data to apparent resistivities and thus a high surface voltage manifests itself in a high

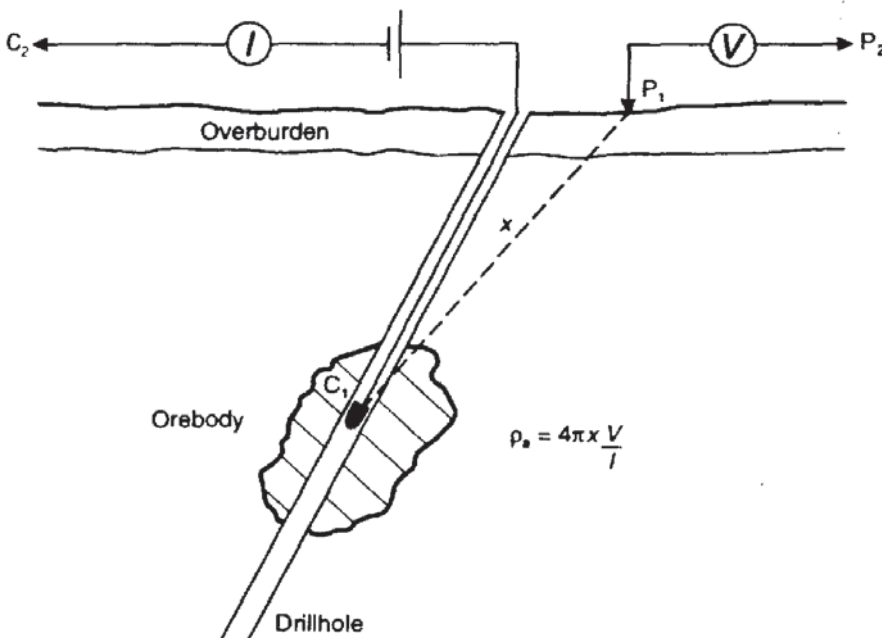


Figure 7.35 Positions of electrodes used in a mise-à-la-masse survey. One form of geometric factor is given where x is the distance between the C_1 electrode down the hole and the P_1 mobile electrode on the ground surface

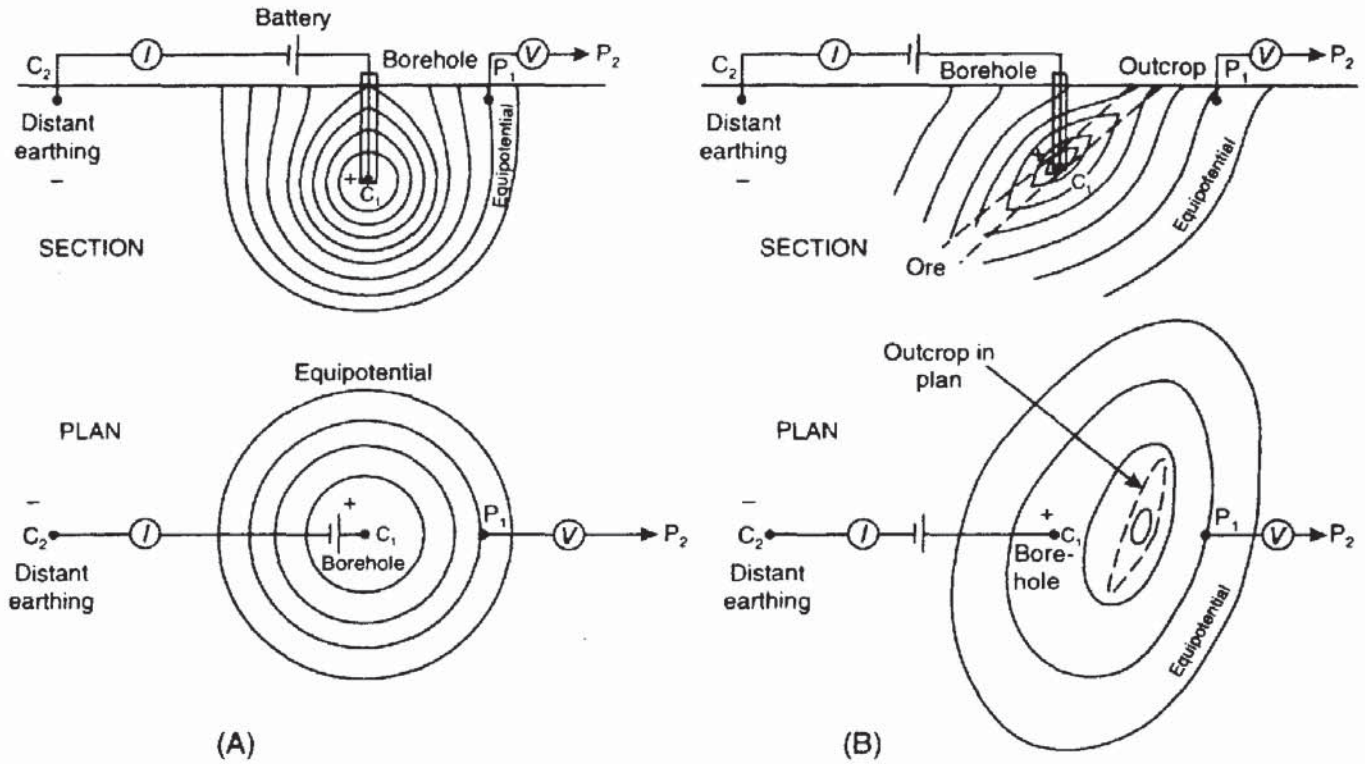


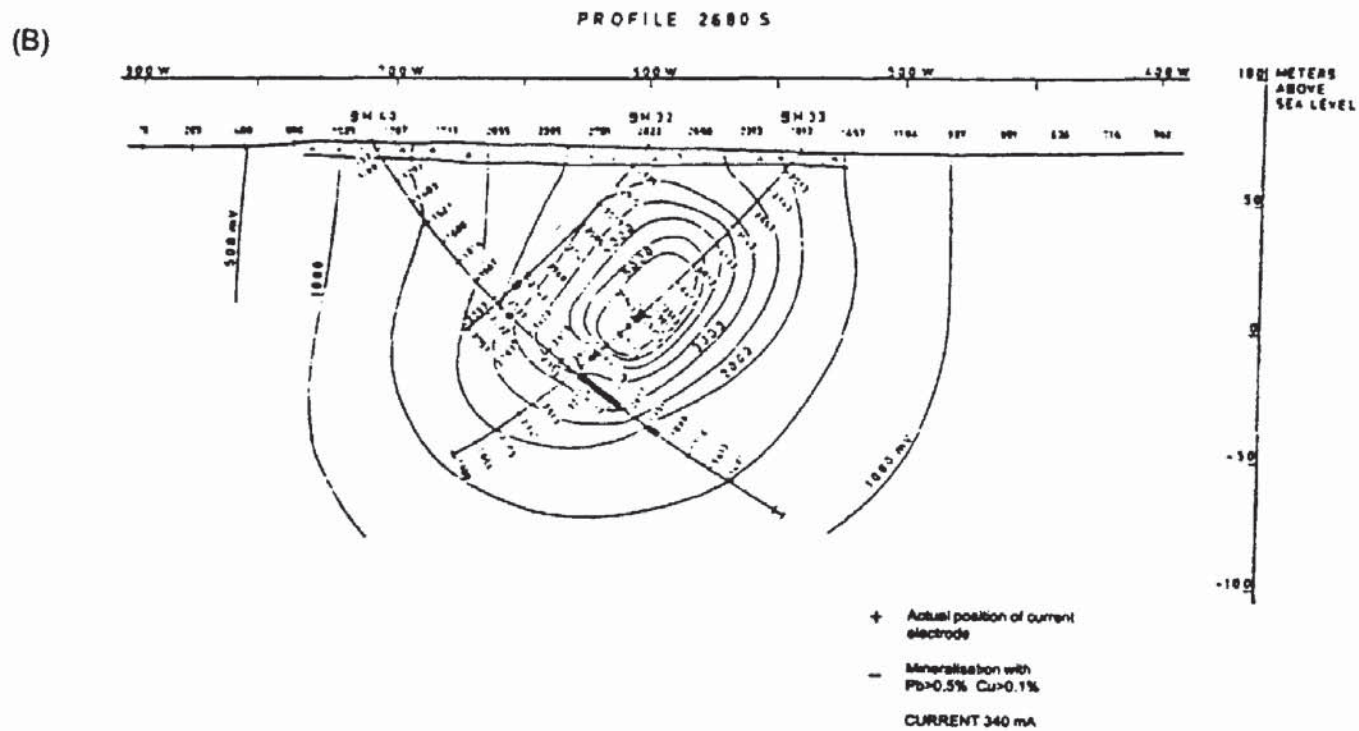
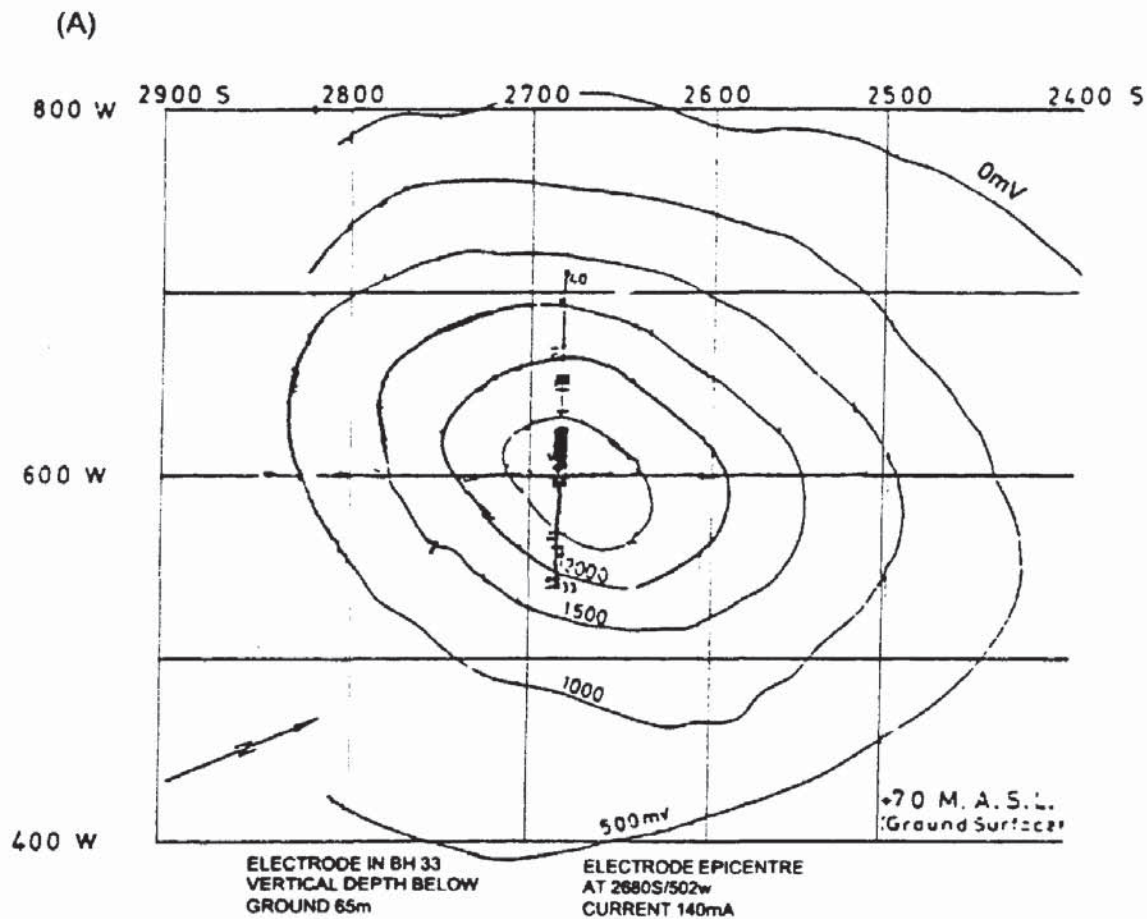
Figure 7.36 (A) Concentric and symmetrical distribution of equipotential lines around a current electrode emplaced within a homogeneous medium. (B) Distortion of equipotentials due to the presence of an orebody. After Parasnis (1966), by permission

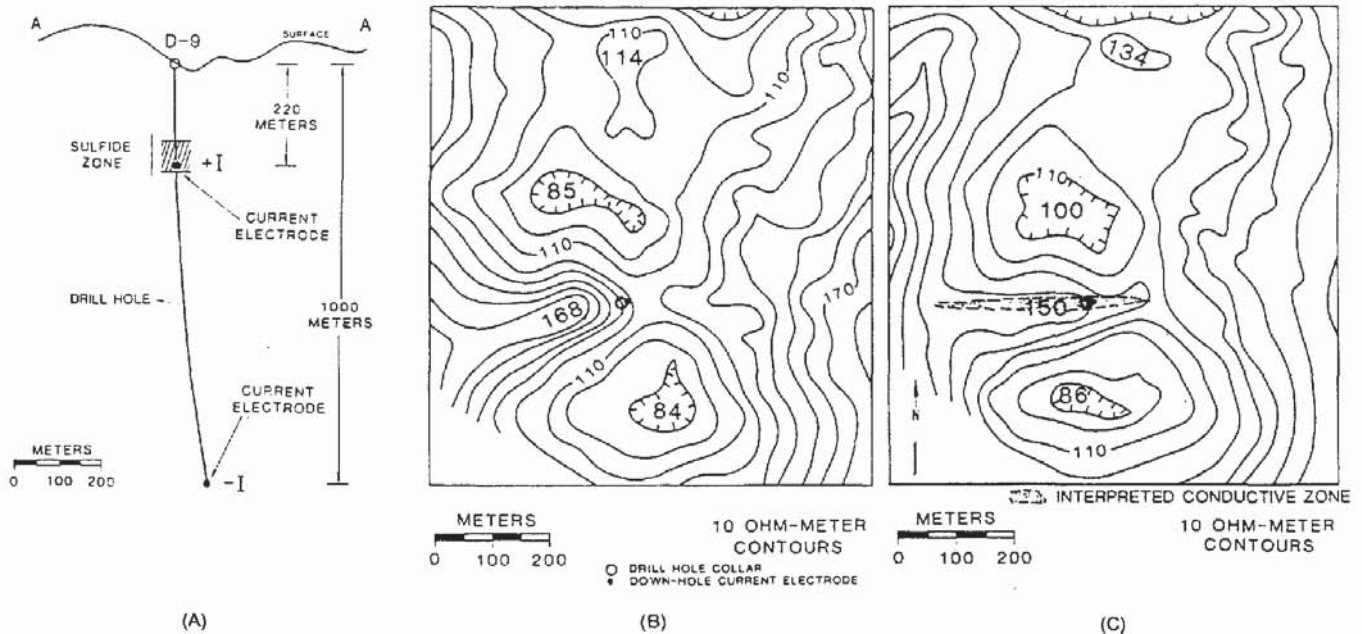
apparent resistivity ($\rho_a = 4\pi x V/I$, where x is the distance between C_1 and P_1).

An example of a *mise-à-la-masse* survey in ore prospecting in Sweden is shown in Figure 7.37. One current electrode was placed 65 m below ground, 89 m down an inclined borehole (borehole 33) and the surface potentials mapped (Figure 7.37A). As there were so many boreholes available in this survey, it was possible to determine the vertical distribution of potentials as well as the surface equipotential distribution (Figure 7.37B). Combining all the available data, it was possible to obtain a three-dimensional image of the potential distribution associated with the target orebody and thus delimit its size, strike and structure (Parasnis 1967).

A second example is shown in Figure 7.38, in which the effects of terrain on the surface potentials can be clearly seen. The positive electrode was placed at 220 m depth down a 1 km deep borehole (Figure 7.38A) and the surface potentials mapped (Figures 7.38B and C). Oppliger (1984) found that when terrain slopes exceeds 10° , surface electric potentials can be adversely affected. The terrain-corrected surface potentials are shown in Figure 7.38C. The main differences are that the low of $85 \Omega m$ and the high of $168 \Omega m$ both change in value (to 100 and $150 \Omega m$ respectively) and, in particular, the orientation of the elongate apparent resistivity high is rotated through 30° . The ridge form of this resistive anomaly suggests that

Figure 7.37 (opposite) (A) Map of surface potentials obtained in a *mise-à-la-masse* survey in Sweden with C_1 in borehole 33. The location of Line 2680S is also shown. (B) Potentials in a vertical section through profile 2680S. From Parasnis (1967), by permission





a conductive body is bounded to the north and south (as indicated by the marked lows) and extends a limited way in an east–west direction. This interpretation has been confirmed by other investigations.

7.7 APPLICATIONS AND CASE HISTORIES

7.7.1 Engineering site investigations

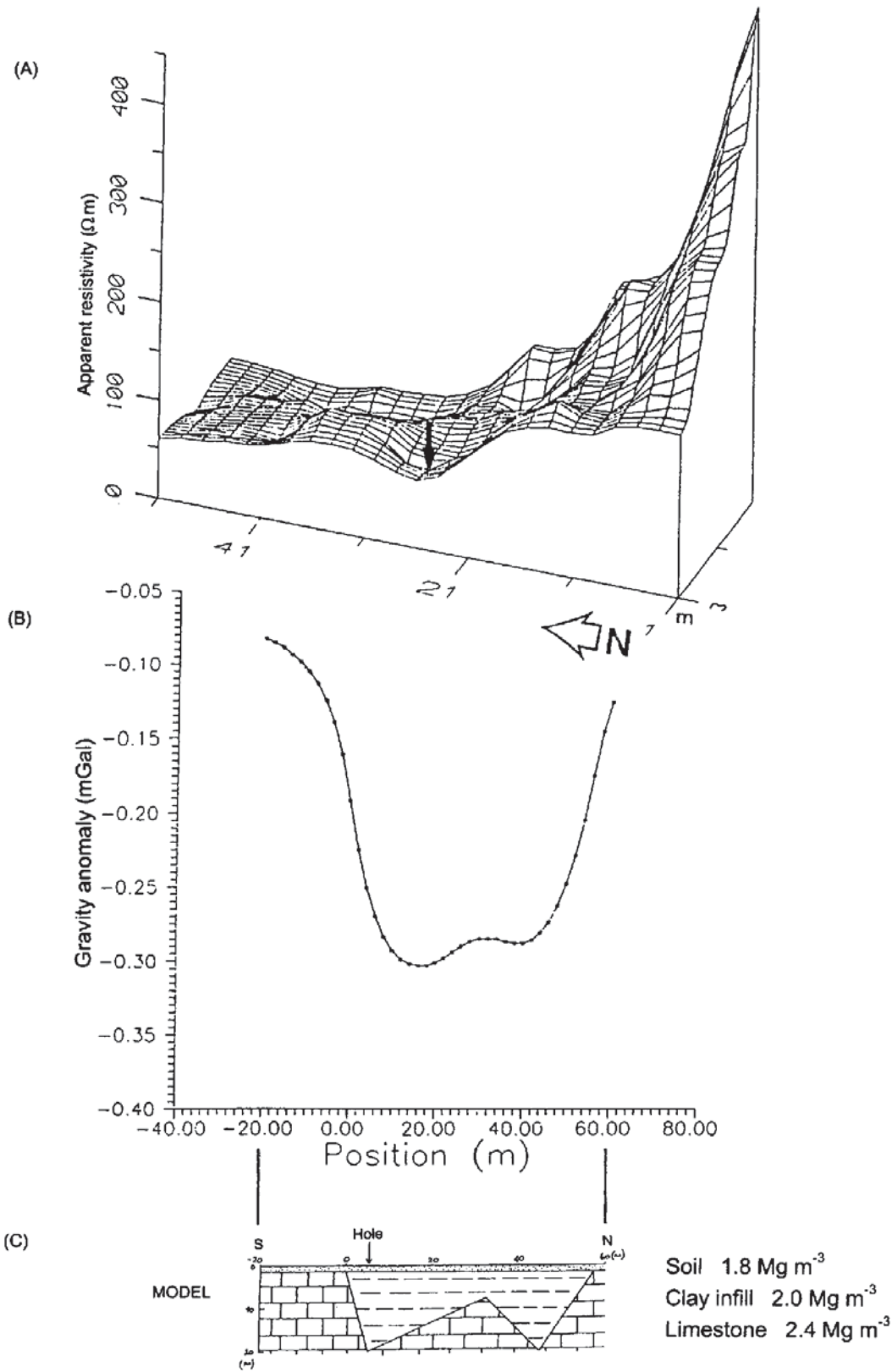
7.7.1.1 *Sub-surface collapse features*

In a small village in east Devon, a 5 m diameter hole appeared overnight in the middle of the road. The local water main had been ruptured and had discharged for over 12 hours and all the water had disappeared down a fissure into underlying limestone. Several of the local buildings started to crack badly, and on investigation it was found that the rafted foundations of several houses had broken and the houses were literally cracking open at the seams, resulting in the emergency evacuation of the residents.

A resistivity survey was initiated in order to determine the sub-surface extent of the problem prior to drilling. Fortunately, the front gardens of the houses affected were all open-plan so there was no difficulty in access, but space was at a premium. A series of constant-separation traverses was instigated using the Wenner array with electrode separations of 10, 15 and 20 m. The resulting apparent resistivity values were plotted as a contour map (Figure 7.39). It was

Figure 7.38 (A) Current electrode configurations. (B) Actual *mise-à-la-masse* apparent resistivities measured on the surface around inclined borehole D-9. Contours are every $10 \Omega \text{ m}$. (C) Terrain-corrected apparent resistivities for the same survey with an interpreted conductive zone indicated. From Oppliger (1984), by permission

Figure 7.39 (*opposite*) (A) Apparent resistivity isometric projection obtained using constant-separation traverses with an electrode separation of 10 m. (B) Modelled microgravity profile that would be expected for the geological model shown in (C): interpreted depth to limestone constrained by drilling. A north–south profile is shown in Figure 7.20. The position of a clay-filled solution feature is arrowed

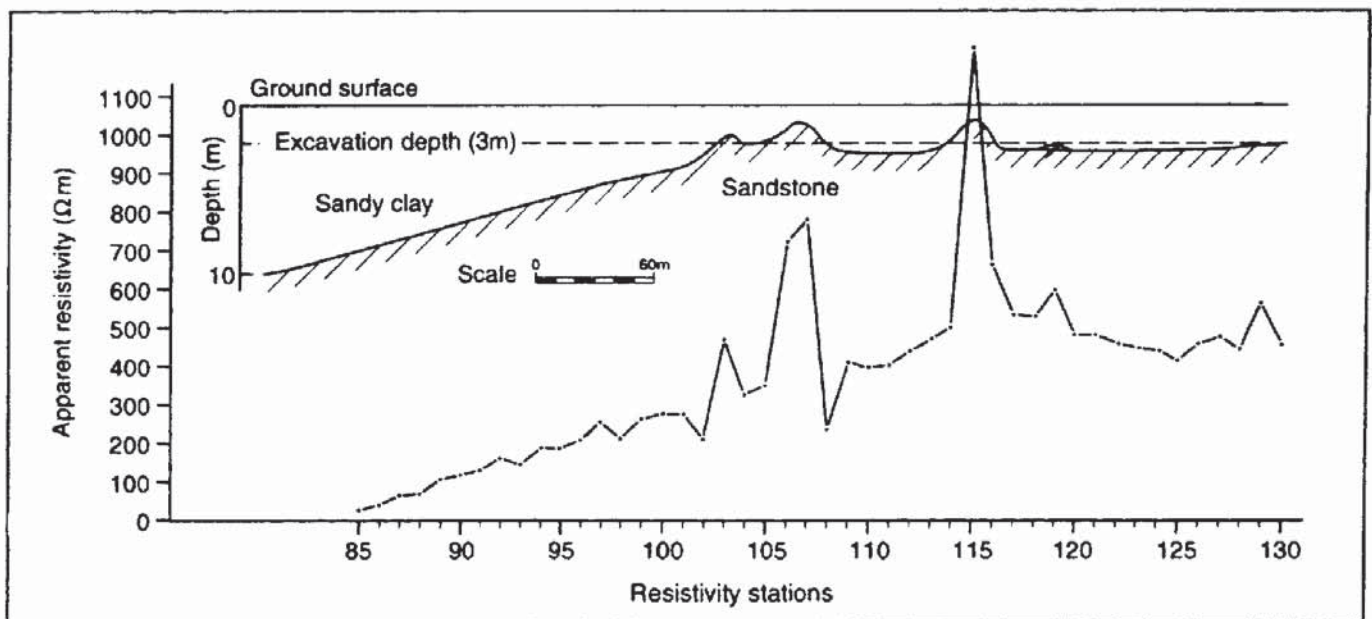


clear that where the hole had appeared, there was a deep infill of clay. It was this that had slipped through a neck of a fissure into a cave beneath, resulting in subsidence beneath the foundations of the houses and the rupture of the water main. The discharging water disappeared into this newly discovered cavern. The clay depth decreased uphill and suddenly increased again, indicating further clay-filled fissures. On drilling these resistivity anomalies, the depth to limestone was confirmed. One drillhole penetrated the cave but failed to locate the bottom; the cave was at least 20 m deep.

7.7.1.2 *Burial of trunk sewer*

A route for a proposed new trunk sewer in South Wales was investigated using electrical resistivity methods because access for drilling equipment was not possible. Both vertical electrical soundings and constant-separation traverses were used along the route and compared with available borehole data from the National Coal Board (Prentice and McDowell 1976). The material through which the sewer trench was to have been dug consisted of superficial deposits overlying Coal Measure sandstone and mudstone. The Coal Measure material was anticipated to be massive and strong and thus hard to excavate, while saturated superficial deposits and Coal Measure shales were thought to provide very unstable trench walls. The CST results using a Wenner array with 10 m electrode separation and 10 m station interval revealed locations where sandstone bedrock was interpreted to be close to the surface which would have required

Figure 7.40 Constant-separation traverse data obtained along the proposed route of a new trunk sewer in South Wales, with the interpreted geological section. After Prentice and McDowell (1976), by permission



blasting for the excavation for the new sewer (Figure 7.40). Seismic refraction was also used to obtain acoustic velocities, which in turn were used to determine whether blasting or ripping techniques should be used in the excavation.

7.7.1.3 Location of permafrost

The presence of massive ground ice and frozen ground provides considerable problems to engineers involved in construction projects. First there are the difficulties in excavation, and secondly, substantial problems can emerge with the thawing of such affected ground. It is therefore vital that ice wedges and lenses, and the extent and degree of permafrost, can be determined well in advance.

Ice has a very high DC electrical resistivity in the range from $1 \text{ M}\Omega \text{ m}$ to $120 \text{ M}\Omega \text{ m}$ (Reynolds and Paren 1984) and therefore forms a particularly resistive target. A variety of geophysical profiles over a proposed road cutting near Fairbanks in Alaska are illustrated in Figure 7.41. Data obtained in the spring show more variability and resolution than when an active layer of thawed ground is present, as in the autumn measurements (Osterkamp and Jurick 1980). Other geophysical methods which are used successfully in this application are electromagnetic profiling, microgravity and ground radar surveying.

7.7.1.4 Location of buried foundations

As part of a trial survey in January 1993, electrical resistivity subsurface imaging was used at a disused railway yard in order to locate old foundations concealed beneath railway ballast. Details of the geophysical survey have been described in more detail by Reynolds and Taylor (1994, 1995) and Reynolds (1995).

The SSI survey was carried out adjacent to a metal chain-link fence and an old diesel tank, and about 3 m from an existing building. It was thought that the remains of two former buildings might still be present beneath the railway ballast and the existing building. The site was totally unsuitable for electromagnetic profiling, because of the above ground structures. It was also unsuitable for ground penetrating radar owing to the coarse ballast and potentially conductive ash also found on site. Despite extremely high electrode contact resistances, a 25 m long array was surveyed with an inter-electrode separation of 1 m. This provided a vertical resolution of 0.5 m or better. The apparent resistivity data were filtered to remove noise spikes and displayed as a pseudo-section (Figure 7.42 A) which was inverted using a deconvolution technique (Barker, personal communication). The final pseudo-section of true resistivities against depth shows a general increase in resistivity with depth (Figure 7.42B). In particular, it revealed two areas of extremely high resistivity ($> 125\,000 \Omega \text{ m}$)

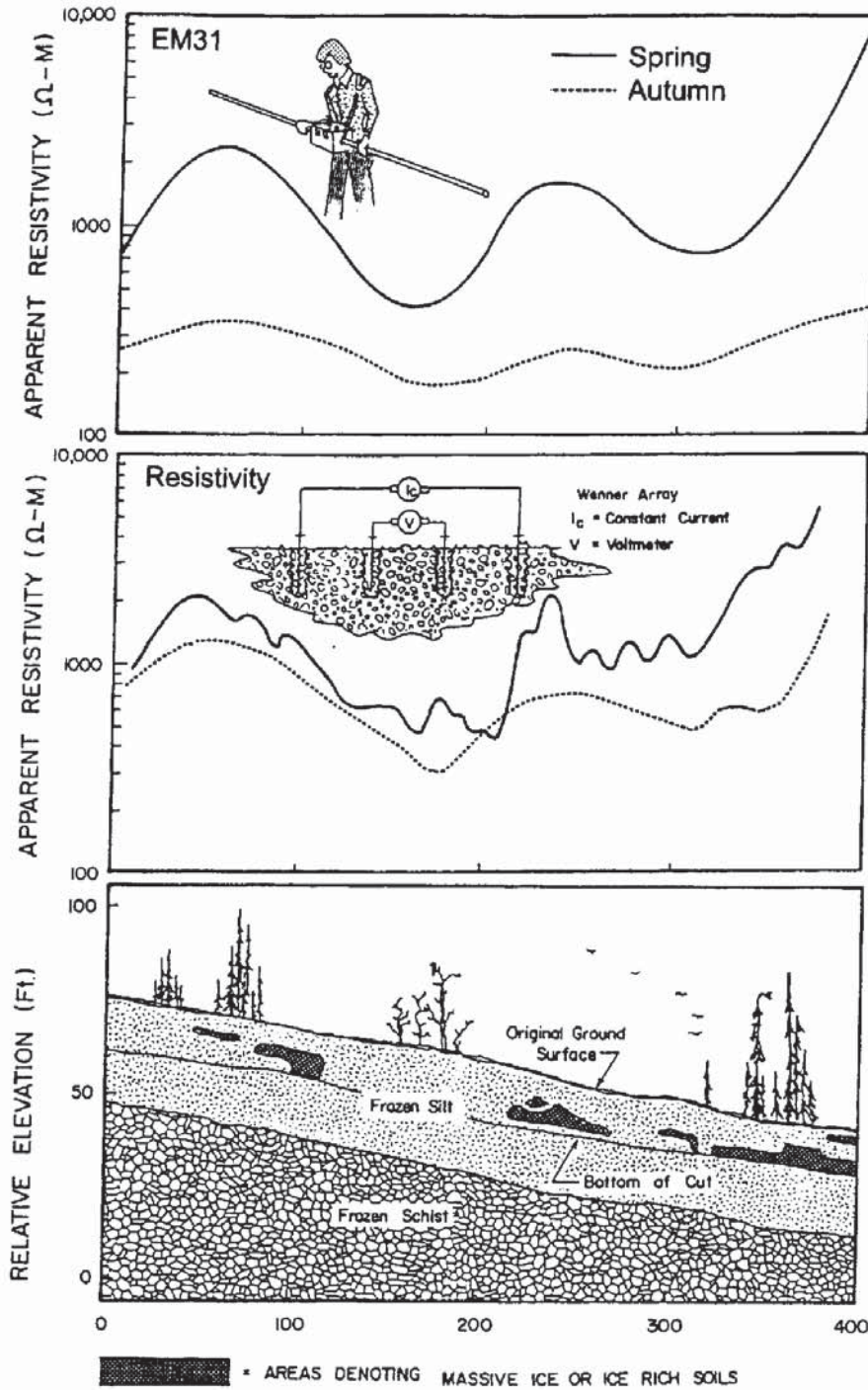
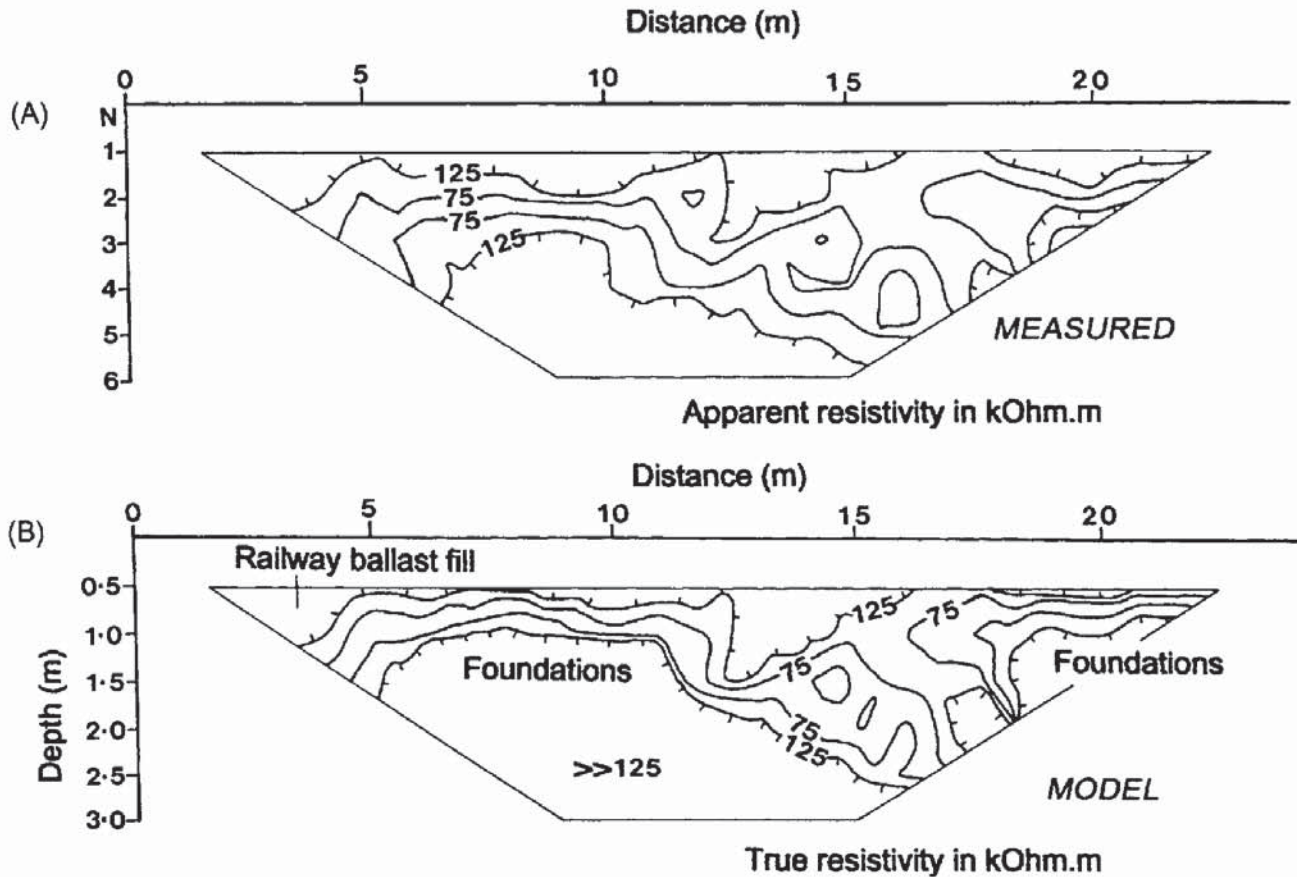


Figure 7.41 Massive ice and frozen ground in a sub-surface profile of a proposed road cut near Fairbanks, Alaska. Also shown are the spring and autumn survey data obtained using electrical resistivity constant-separation traversing and electromagnetic induction (EM31). Massive ground ice produces significant apparent resistivity highs. From Osterkamp and Jurick (1980), by permission

at a depth of about 1 m which had very flat tops to the anomalies. These were interpreted to be due to buried foundations. The main anomaly (between 6 and 11 m along the array) was found to correlate with the outline of one former building on an old plan. The second feature (starting at around 18 m) is thought to be due to the other old building. However, the location was found to be several metres further away from the first building than indicated on the plans. The



depth to the foundation was thought to be reasonable as adjacent brick slabs excavated a few metres away were found at a comparable depth.

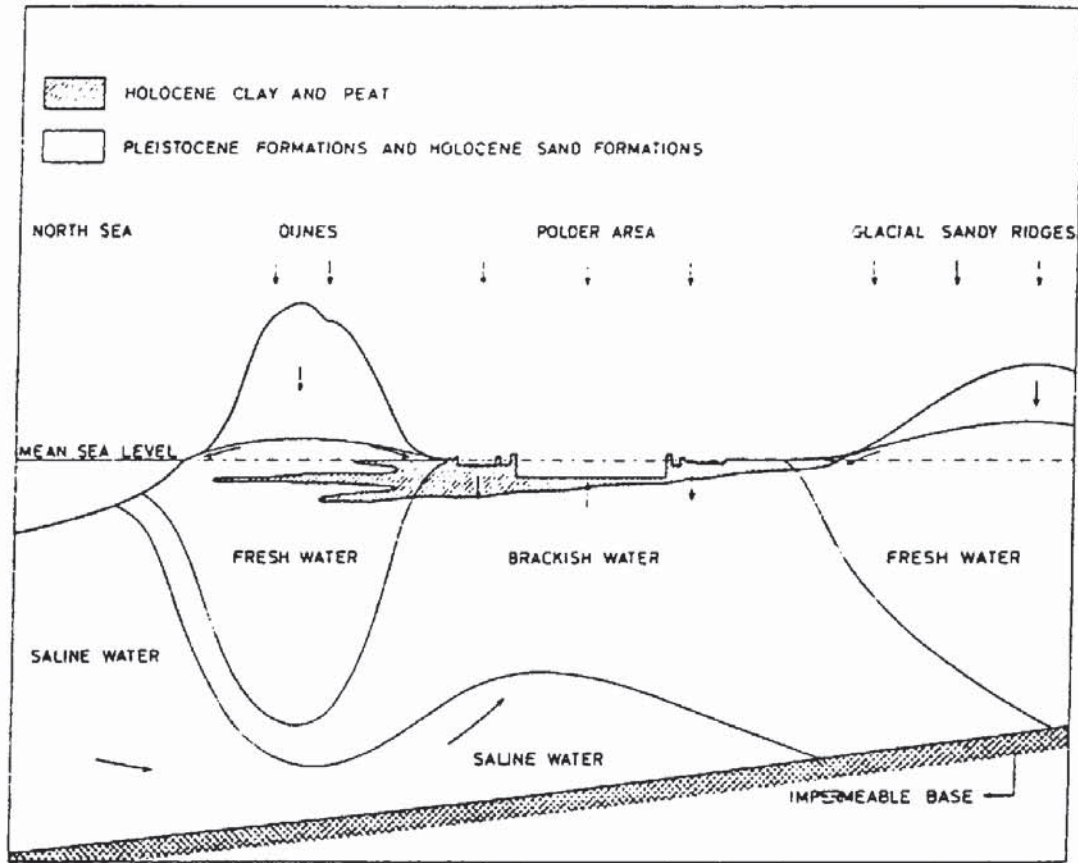
Figure 7.42 Electrical resistivity subsurface imaging pseudo-sections: (A) apparent resistivity profile, and (B) true resistivity–depth profile, over buried concrete slabs at 1 m depth. From Reynolds and Taylor (1995), by permission

7.7.2 Groundwater and landfill surveys

7.7.2.1 Detection of saline groundwater

In the mid-1950s, a comprehensive electrical resistivity survey programme was initiated in order to map out saline groundwater in areas of the Netherlands below or at mean sea level. Figure 7.43 shows schematically the nature of the hydrogeology in the western part of the Netherlands. The vertical electrical soundings provided a means of obtaining information about the vertical distribution of fresh, brackish and saline water bodies and their areal extent (Figure 7.44).

Pockets of saline water were found which were thought to be remnants from before the fifteenth century after which time the present sea-dyke formed, cutting off the sea. To the west of Alkmaar, some 30 m of saline water was found above tens of metres of fresh water separated by an impermeable clay layer. Major demands for construction sand for the building of new roads and urbanisation

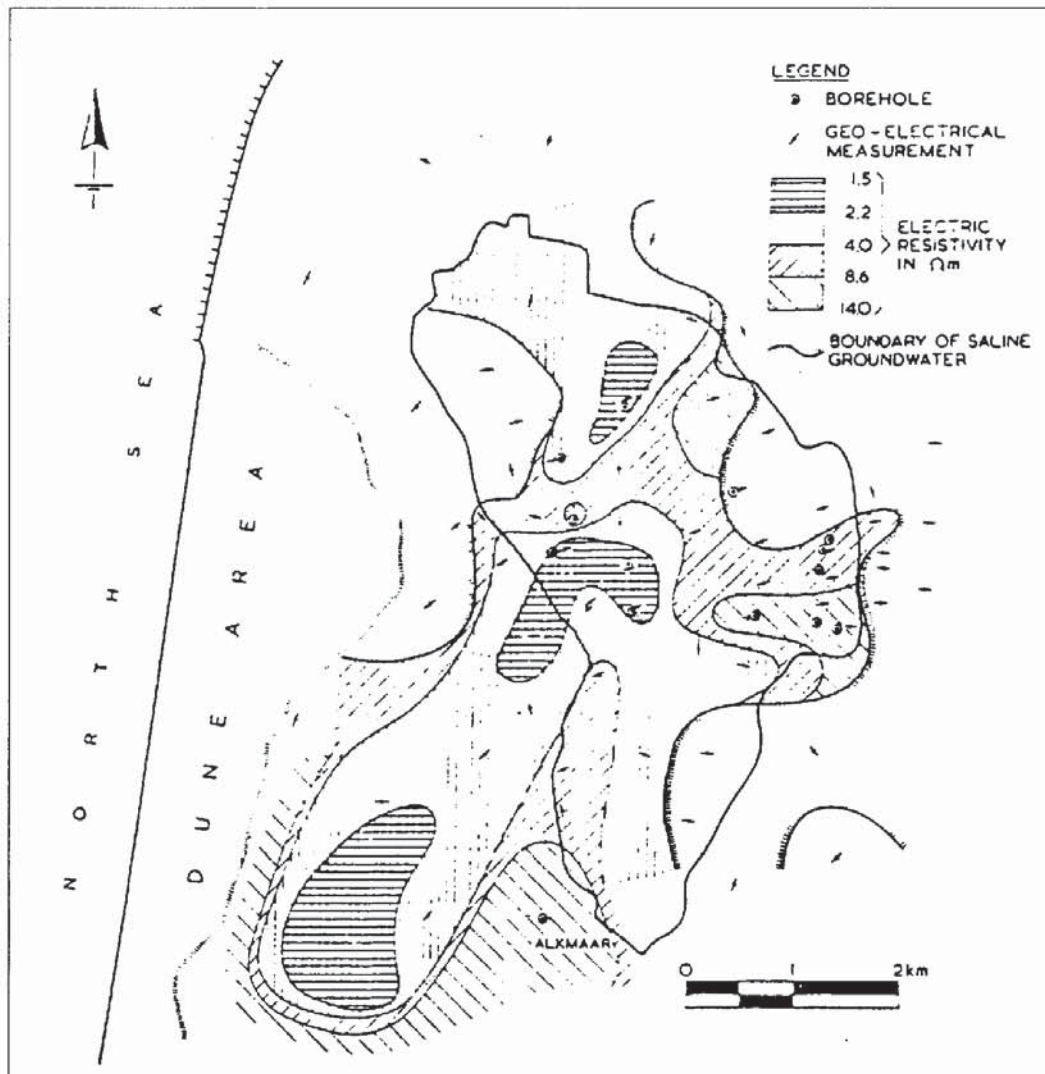


could have led to the extraction of sands with the demise of the clay barrier. This could have resulted in the mixing of the water bodies and the contamination of an otherwise potable water supply. Furthermore, correlation of resistivities from modelling of VES data with borehole information about groundwater chemistry has led to a relationship between chloride content and resistivity. Consequently, it is possible to determine chloride content of the groundwater from the resistivity data.

Figure 7.43 Schematic hydrogeological cross-section for the western part of the Netherlands. From van Dam and Meulenkamp (1967), by permission

7.7.2.2 *Groundwater potential*

In Kano state, northern Nigeria, an internationally funded aid programme was established in the 1980s to provide tubewells with handpumps for 1000 villages in rural areas. Village populations ranged from several hundred to no larger than 2000 people, but all were in very remote locations. Failure to obtain a reliable supply of water would have resulted in many of the villages being abandoned and the populations moving to the larger towns, thereby compounding the local problems of sanitation and health, education and employment, and the demise of rural culture and skills.



It was first recommended that geophysics was unnecessary to locate groundwater; boreholes drilled anywhere would succeed. In practice, borehole failures were in excess of 82% of holes drilled, particularly in the southern areas. Geophysical methods were then called upon to improve the failure rate. Predominantly, vertical electrical soundings were used on sites selected following initial hydrogeological and photogeological inspection. Careful analysis of the VES data with the subsequent borehole information, led to the compilation of a database of typical formation resistivities and their likely hydrogeological potential. It became apparent that certain geographical regions had better and more easily resolved groundwater resources, and six drilling rigs were kept working on these sites. This provided a window of several months in which the more problematic sites could be investigated further until they, too, were ready for drilling.

Figure 7.44 Distribution of resistivities of a sand layer with a saline groundwater boundary in Noord Holland as determined by many vertical electrical soundings. From van Dam and Meulenkaamp (1967), by permission

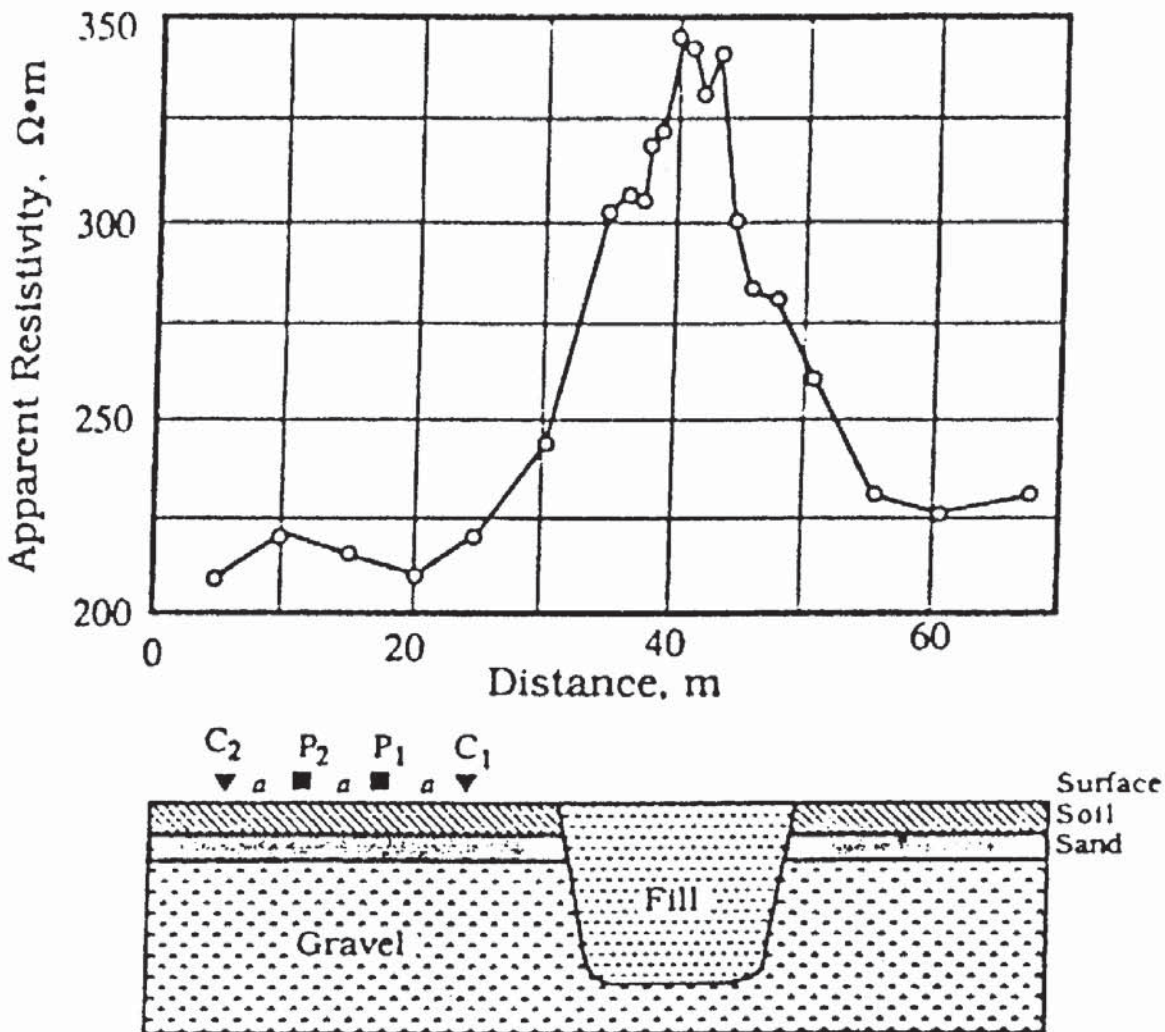
Use of geophysics to help identify the groundwater potential in areas and to assist in the planning of drilling programmes led to the borehole failure rate falling to 17% of holes drilled and a saving to the project of £5 million – at least 10 times the cost of the geophysical surveys (Reynolds 1987).

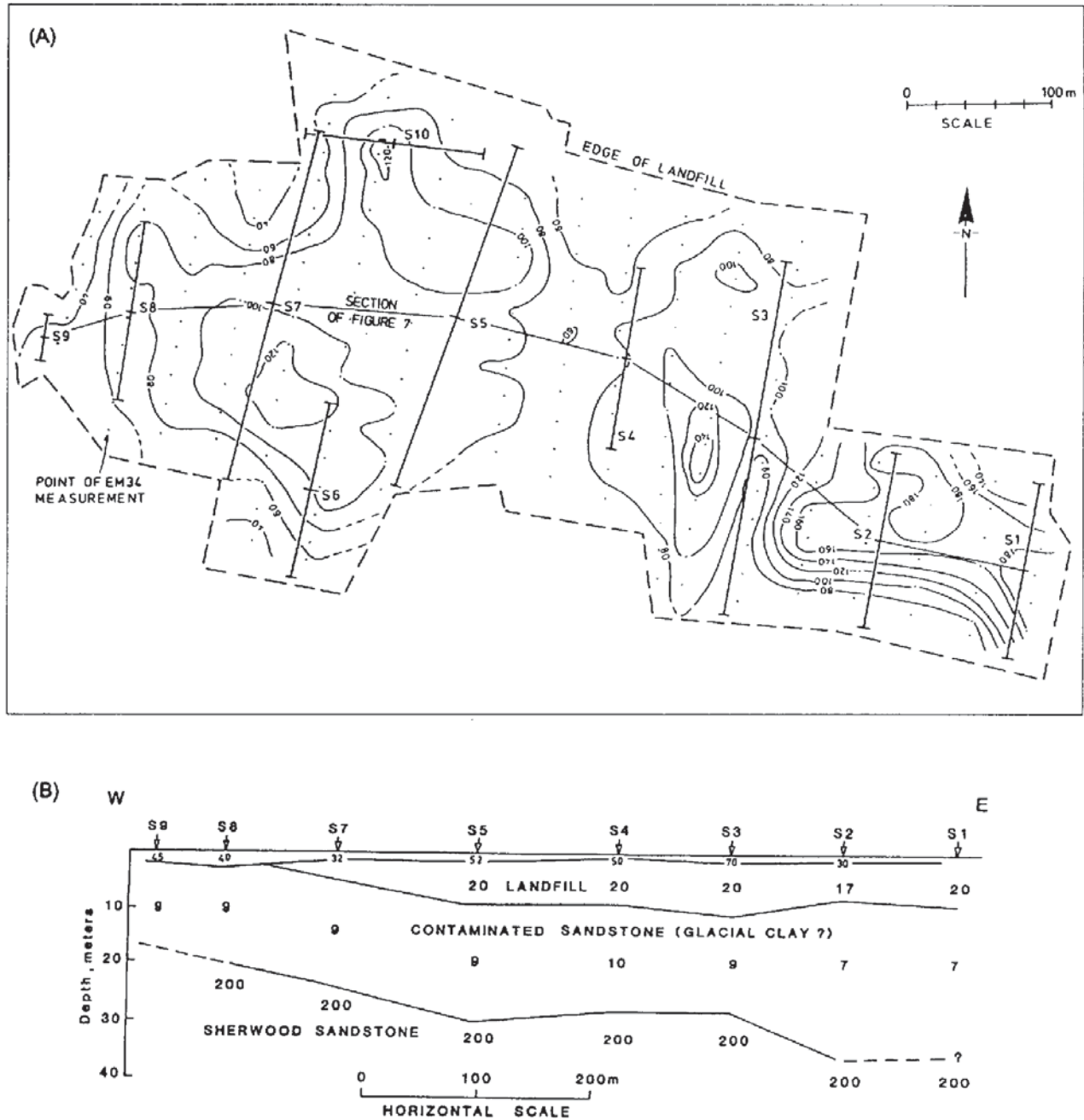
7.7.2.3 Landfills

There is an increasing amount of interest in the use of high-resolution resistivity surveys in the investigation of closed landfills, particularly with respect to potential leachate migration. Both resistivity sounding and sub-surface imaging have been used very successfully.

There is no such thing as a typical landfill – some are extremely conductive, others are resistive relative to the surrounding media. There are many variables geophysically (Reynolds and McCann 1992) and care must be taken not to presume a particular geophysical response for any given site. For example, van Nostrand and Cook

Figure 7.45 Observed apparent resistivity profile across a resistive landfill using the Wenner array. From van Nostrand and Cook (1966), by permission





(1966) presented a very clear CST profile of apparent resistivity across a resistive landfill (Figure 7.45). Barker (1990) has shown resistivity sounding results across a landfill in Yorkshire in which the landfill is conductive (around 20 Ω m or less) over a contaminated substrate of sandstone (Figure 7.46). The offset Wenner method was used in this example.

Schlumberger soundings have been used by Monier-Williams *et al.* (1990) as part of a broader geophysical survey around the Novo Horizonte landfill in Brazil. Quantitative analysis of the soundings

Figure 7.46 (A) Contoured ground conductivity values over a landfill. Solid straight lines represent the positions and orientations of resistivity soundings. Contour interval is 20 ms/m. (B) Geoelectrical section across the landfill based on the soundings in (A). From Barker (1990), by permission

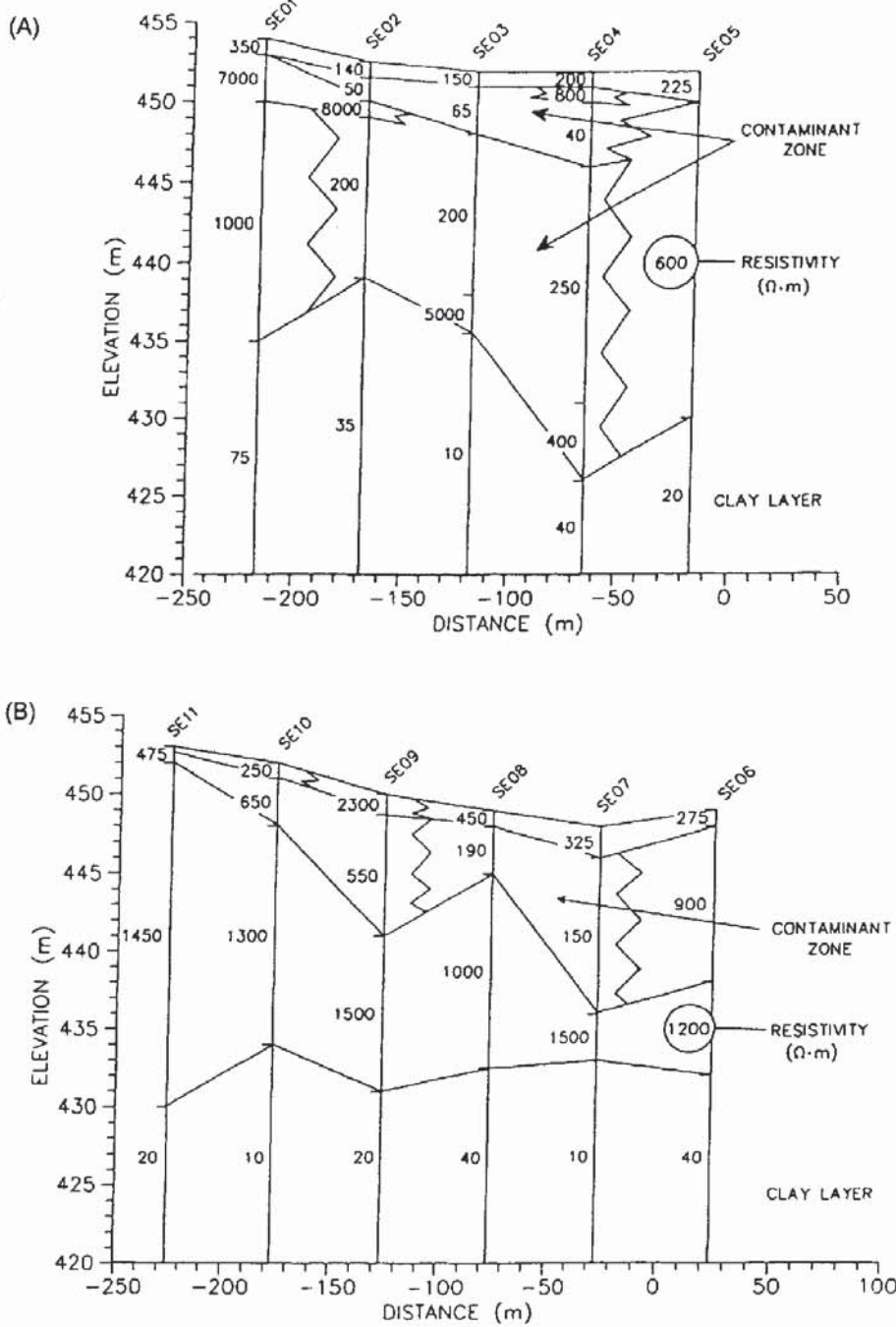
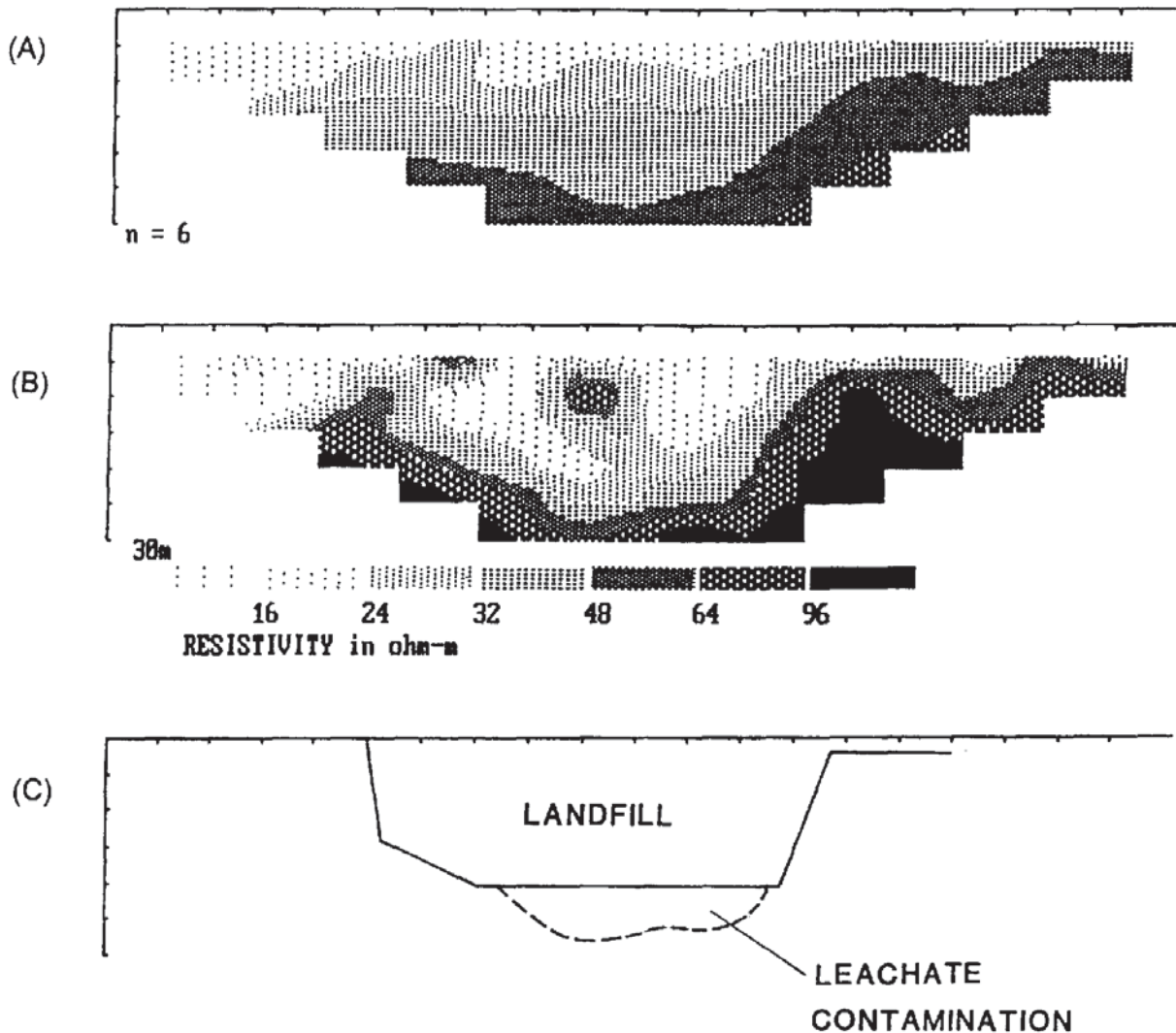


Figure 7.47 Two parallel resistivity sections based on the interpretation of Schlumberger soundings at the Novo Horizonte landfill site, Brazil. The profile in (A) is closer to the landfill than that shown in (B). The background resistivities above the basal clay are high; the lower values in the centre of the sections are assumed to be due to contamination. Note that the conductive zone in (B) is apparently more shallow than in (A). From Monier-Williams *et al.* (1990), by permission

and displays as resistivity panels have revealed significant zones with anomalously low resistivities (Figure 7.47). These have been interpreted as being contaminant plumes arising from the landfill. The displays shown in the figure are orientated parallel to the flank of the landfill, but at 10 m and 70 m distance away from it.

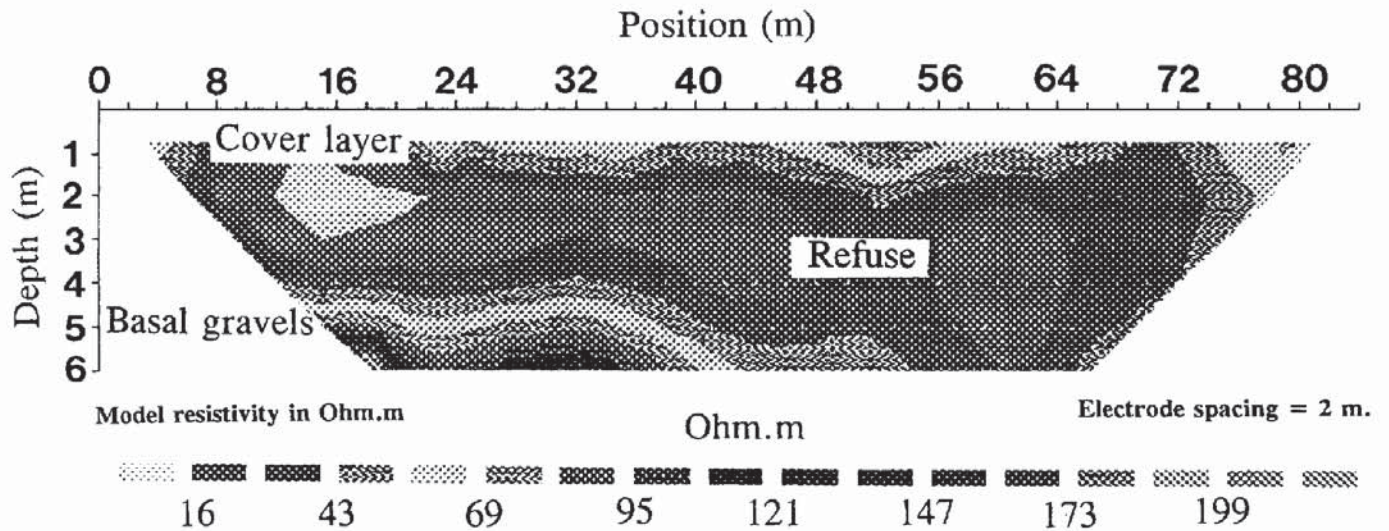
Sub-surface imaging pseudo-sections across a landfill are shown in Figure 7.48. The three panels illustrate the observed apparent



resistivity data, the inverted true resistivity–depth model and a schematic interpretation. In this case, the depth and geometry of the landfill were known at the outset. The zone of low resistivity associated with the saturated landfill extends more deeply than had been expected. This is interpreted as indicating the leakage of leachate through the base of the landfill (Barker 1992).

A further example of a sub-surface imaging pseudo-section inverted model is shown in Figure 7.49 (Reynolds 1995). The data were acquired over a closed shallow landfill constructed as a ‘dilute and disperse’ site over river gravels. The electrical image shows the thin capping material, the waste material and the basal gravels quite clearly. The image is entirely consistent with depths known from boreholes on site.

Figure 7.48 (A) Wenner apparent resistivity pseudo-section measured across a landfill. Electrode spacing = 10 m. (B) Resistivity depth section obtained after eight iterations. (C) Approximate section across the landfill based on existing information. From Barker (1992), by permission



7.7.3 Glaciological applications

Electrical resistivity methods have been used since 1959 to determine glacier ice thickness. Measurements were first obtained on European glaciers on temperate ice (i.e. ice at its pressure melting point). In 1962, resistivity measurements were made on polar ice (i.e. ice well below its pressure melting point) and were found to be anomalously low by up to three orders of magnitude compared with temperate ice values. Whereas the electrical resistivity behaviour of polar ice is now reasonably understood (Figure 7.50; Reynolds and Paren 1984), the electrical behaviour of temperate ice is still poorly understood. In the 1970s a considerable amount of work was undertaken to develop field data acquisition in Antarctica. Interpretation methods were developed to yield information on vertical thermal profiles through the ice mass and whether or not ice shelves afloat on sea water were melting or freezing at their base. All of these data contribute to an understanding of ice dynamics (rate of ice movement, etc.) and the structure of the ice masses under study.

A series of vertical electrical soundings has been made on George VI Ice Shelf along a flow line of Goodenough Glacier which flows westwards from the Palmer Land Plateau in the Antarctic Peninsula (Figure 7.51). The field curves were modelled to take into account thermal effects and the resulting interpretations are shown in Figure 7.52. The estimated ice thicknesses and rates of bottom melting were in good agreement with those determined independently (Reynolds 1982).

Figure 7.49 Electrical resistivity pseudo-section acquired over a closed landfill in north Wales. From Reynolds (1995), by permission